Journal of
Chemical Engineering & Process Technology

Dzulkifli et al., J Chem Eng Process Technol 2017, 8:3
DOI: 10.4172/2157-7048.1000336

Research Article Open Access

Soret and Dufour Effects on Unsteady Boundary Layer Flow and Heat Transfer of Nanofluid Over a Stretching/Shrinking Sheet: A Stability Analysis

Nor Fadhilah Dzulkifli[1,2], Norfifah Bachok[2], Ioan Pop[3*], Nor Azizah Yacob[1], Norihan Md Arifin[2] and Haliza Rosali[2]

[1]*Department of Mathematics, Faculty of Computer and Mathematics Sciences, Universiti Teknologi MARA Pahang, Bandar Pusat Jengka, Pahang, Malaysia*
[2]*Department of Mathematics and Institute for Mathematical Research, Universiti Putra Malaysia, UPM Serdang, Selangor, Malaysia*
[3]*Department of Mathematics, Babes-Bolyai University, Cluj-Napoca, Romania*

Abstract

The effects of Soret and Dufour parameters on the boundary layer flow in nanofluid over stretching/ shrinking with time dependent is studied using Buongiorno model. The system of partial differential equations is transformed to the system of ordinary differential equations by applying similarity transformation. The results are obtained numerically using bvp4c in Matlab. The reduced skin friction coefficient reduced Nusselt number, velocity, temperature and concentration profiles are shown graphically with different values of Soret effect, Dufour effect, mass flux parameter, unsteadiness parameter, thermophoresis as well as Brownian motion parameter where the dual solutions are obtained. The unsteadiness parameter and mass flux parameter expand the range of solution for stretching/ shrinking parameter. Meanwhile, the Soret and Dufour parameters are found to affect the heat transfer rate at the surface. In order to determine the stability of the solutions, stability analysis is performed.

Keywords: Unsteady boundary layer; Nanofluid; Soret effect; Dufour effect; Heat transfer; Stability analysis

Nomenclature

A unsteadiness parameter

C nanoparticle volume fraction

C_f skin friction coefficient

C_∞ ambient fluid concentration

C_s concentration susceptibility

D_B Brownian diffusion coefficient

D_f Dufour number

D_m coefficient of mass diffusivity

f dimensionless stream function

k thermal conductivity

Le Lewis number

Nb Brownian motion parameter

Nt thermophoresis parameter

Nu_x local Nusselt number

p fluid pressure

Pr Prandtl number

q_w surface heat flux

Re_x local Reynolds number

s mass flux parameter

Sr Soret number

t time

T fluid temperature

T_w plate temperature

T_∞ ambient temperature

T_m mean fluid temperature

u,v velocity components along the x and y directions, respectively

u_w velocity of the plate

v_w velocity of mass flux

x,y Cartesian coordinates along the surface and normal to it, respectively

Greek symbols

α thermal diffusivity

γ eigenvalue

η similarity variable

θ dimensionless temperature

ε stretching/ shrinking parameter

μ dynamic viscosity

ν kinematic viscosity

ϕ nanoparticle volume fraction parameter

ρ fluid density

***Corresponding author:** Ioan Pop, Department of Mathematics, Babes-Bolyai University, Cluj-Napoca, Romania, Tel: 0722218681; E-mail: popm.ioan@yahoo.co.uk

Received April 30, 2017; **Accepted** May 09, 2017; **Published** May 20, 2017

Citation: Dzulkifli NF, Bachok N, Pop I, Yacob NA, Arifin NM, et al. (2017) Soret and Dufour Effects on Unsteady Boundary Layer Flow and Heat Transfer of Nanofluid Over a Stretching/Shrinking Sheet: A Stability Analysis. J Chem Eng Process Technol 8: 336. doi: 10.4172/2157-7048.1000336

$(\rho c_p)_{nf}$ heat capacity of the nanofluid

$(\rho c_p)_p$ heat capacity of the nanoparticle

τ_w surface shear stress

ψ stream function

Subscripts

w condition at the surface of the surface

∞ ambient condition

nf nanofluid

p nanoparticle

f basefluid

Superscript

Differentiation with respect to η.

Introduction

Generally, it was known that heat and mass fluxes were created from temperature and concentration gradient, respectively. However, heat flux is actually can existed due to the concentration gradient which is known as Soret effect. Same goes to the mass flux where the flux occurred by the temperature gradient and is called Dufour effect. Configuration involving the heat and mass transfer with Soret and Dufour effects is an important subject due to a wide range of applications such as the solidification of binary alloys, groundwater pollutant migration, chemical reactors, geosciences multi-component melts, oil-reservoirs, isotope separation, and in mixture between gases. Generally, the effects of diffusion of matter caused by temperature gradients (Soret effect) and diffusion of heat caused by concentration gradients (Dufour effect) can be become influential when the temperature and concentration gradients are very large. Joly et al. [1] analyzed the thermal and solutal effects on natural convection in a vertical enclosure. Mansour et al. [2] have obtained a multiplicity of solutions induced by thermosolutal convection in a square porous cavity with horizontal concentration gradient in the presence of Soret effect. Chamkha and Rashad [3] studied the Soret and Dufour effects on unsteady double-diffusive convection flow from a rotating vertical cone with chemical reaction effects. Kafoussias and Williams [4] investigated the effects of Soret and Duffour on mixed convection and mass transfer laminar boundary layer flow over a vertical flat plate. Besides Soret and Dufour effects, Alam et al. [5] has considered suction variable on mixed convection flow over a semi-infinite vertical porous flat plat and they found that the wall suction stabilized the boundary layer growth of velocity, temperature and concentration. Similar to Alam et al. [5], El-Kabeir [6] also considered the porous medium in the study but he considered stretching cylinder rather than flat plate. In addition, the effect of chemical reaction was also investigated in the work.

Low thermal conductivity of working fluids such as water, mineral oils, ethylene glycol is a primary limitations of enhancing the heat transfer performance. To avoid this situation to add high thermal conductivity of nanoparticles in the working fluid. Due to the excellent thermal property, nanofluids are used in the areas of building heating, heat exchangers, and the automotive cooling process. The term of nanofluid first introduced by Choi [7] in 1995 is one of the mean to improve or enhance the thermal conductivity, which is proportional to heat transfer of the conventional regular fluid such as water, ethylene glycol and mineral oil. Basically, these regular fluids have low thermal conductivity and by dispersing nanoparticles in the base fluid, the thermal conductivity of the fluid can be enhanced. Several works are concerned with natural convection filled with nanoparticles, Khanafer et al. [8], Tiwari and Das [9], Oztop and Abu-Nada [10], who concluded that the Cu-water based nanofluid has the higher heat transfer rate compared with other nanofluids. Lai and Yang [11], Aminossadati and Ghasemi [12] reported that increase the solid volume fraction of the nanoparticles yields a increasing value of heat transfer.

Buongiorno [13] proposed a model for momentum, heat and mass transfer in nanofluid where this model focussed on two slip mechanism that can produced relative velocity between nanoparticles and regular fluid which were Brownion diffusion and thermophoresis. Buongiorno model has been used by Kuznetsov and Nield [14] to study the natural convective boundary layer flow passing through a vertical plate in nanofluid. Meanwhile, different boundary layer condition has been applied in the model by Mansur and Ishak [15], Kuznetsov and Nield [16]. Some of the authors studied the effect of nanouids for the case of mixed convection Nemati et al. [17], Cimpean and Pop [18], etc. Very good literature reviews on convective flow and applications of nanofluids have been done by Jou and Tzeng [19], Das et al. [20], Kleinstreuer et al. [21], Kakaç and Pramuanjaroenkij [22], Wong and Leon [23], Wen et al. [24], Jaluria et al. [25], Mahian et al. [26], Nield and Bejan [27], Sheikholeslami and Ganjii [28], and Shenoy et al. [29] have given reviews of nanofluid on natural convection heat transfer.

Recently, the stability analysis is important to be performed when there are more than one solution exists in order to determine the stability of the solutions. The analysis can be obtained by adopting the work proposed by Merkin [30]. According to According to Ishak [31] the implementation of the analysis was to investigate the growth of disturbances for first and second solutions where the solution with initial decay of disturbance represented the stable solution, while the solution with initial growth of disturbance indicated the unstable solution. There were some authors who performed the analysis in their studies over various cases such as Weidman et al. [32]. Aleng et al. [33], Nazar et al. [34], Hafidzuddin et al. [35], Bachok et al. [36] and Najib et al. [37] studied several problems on stretching/shrinking sheet in a viscous and incompressible fluids and they found that the first solution was stable while the second solution was unstable. It is worth mentioning that the flow caused by a stretching/shrinking surface gets up mostly in the field of chemical engineering and metallurgy such as aerodynamic and polymer extrusion, cooling of metallic plate, drawing of paper films, glass blowing, and paper production.

The present study is an extension of Bachok et al. [38] with new boundary condition proposed by Kuznetsov and Nield [16]. The main purpose of this present work is to investigate the boundary layer flow and heat transfer characteristics over a stretching/ shrinking sheet in nanofluid when the Soret and Dufour effects are taken into consideration for unsteady problem. The governing equations are transformed to ordinary differential equations using dimensionless similarity transformation parameter and are solved numerically by Matlab. The stability analysis is performed in order to determine the stability of the numerical solutions.

Problem Formulation

Unsteady boundary layer flow over a stretching/ shrinking surface immersed in nanofluid is considered. At $t<0$, it is assumed that the surface is in stationary state with velocity $\mu_{w=0}$. As $t>0$, the surface begin to stretch or shrink where the velocity of the sheet is $\mu_{w=}Ax / t$ which $A>0$ is dimensionless acceleration parameter. The velocity of mass flux is represented by v_w where $v_w>0$ is for injection and $v_w<0$ is for suction. Let

the uniform temperature of the plate is T_w T_∞ and C_∞ are the temperature and the nanoparticle volume fraction of the ambient fluid. Following the assumptions above, the governing equations of the problem are, see Bachok et al. [38], and Alam et al. [5],

$$\frac{\partial u}{\partial x}+\frac{\partial v}{\partial y}=0, \tag{1}$$

$$\frac{\partial u}{\partial t}+u\frac{\partial u}{\partial x}+v\frac{\partial u}{\partial y}=-\frac{1}{\rho}\frac{\partial p}{\partial x}+\nu\frac{\partial^2 u}{\partial y^2}, \tag{2}$$

$$\frac{\partial v}{\partial t}+u\frac{\partial v}{\partial x}+v\frac{\partial v}{\partial y}=-\frac{1}{\rho}\frac{\partial p}{\partial y}+\nu\frac{\partial^2 v}{\partial y^2}, \tag{3}$$

$$\frac{\partial T}{\partial t}+u\frac{\partial T}{\partial x}+v\frac{\partial T}{\partial y}=\alpha\frac{\partial^2 T}{\partial y^2}+\tau\left[D_B\frac{\partial C}{\partial y}\frac{\partial T}{\partial y}+\frac{D_T}{T_\infty}\left(\frac{\partial T}{\partial y}\right)^2\right]+\frac{D_B k_T}{c_s c_p}\frac{\partial^2 C}{\partial y^2}, \tag{4}$$

$$\frac{\partial C}{\partial t}+u\frac{\partial C}{\partial x}+v\frac{\partial C}{\partial y}=D_B\frac{\partial^2 C}{\partial y^2}+\frac{D_T}{T_\infty}\frac{\partial^2 T}{\partial y^2}+\frac{D_B k_T}{T_m}\frac{\partial^2 T}{\partial y^2}, \tag{5}$$

subject to boundary conditions (see Kuznetsov and Nield [16])

$t<0$, $v=0$, $u=0$, $T=T_\infty$, $C=C_\infty$ for all x and y,

$$t\geq 0,\ v=v_w,\ u=u_w(x)=\varepsilon\frac{Ax}{t},\ T=T_w,\ D_B\frac{\partial C}{\partial y}+\frac{D_T}{T_\infty}\frac{\partial T}{\partial y}=0 \quad \text{at } y=0, \tag{6}$$

$u\to 0$, $T\to T_\infty$, $C\to C_\infty$ as $y\to\infty$,

Where x and y are the Cartesian coordinate along and perpendicular to the plate with u and v are the velocity component in x and y directions, respectively, T is the temperature of the nanofluid, C is the nanoparticle fraction, v is the kinematic viscosity of the nanofluid, α is the thermal diffusivity of the nanofluid, ρ is the fluid pressure, D_B is the Brownian diffusion coefficient, D_T is the thermophoretic diffusion coefficient, D_m is the coefficient of mass diffusivity, C_p is the specific heat at constant pressure, T_m is the mean fluid temperature, k_T is the thermal diffusion ratio, C_s is the concentration susceptibility, $\tau=(\rho c_p)_f/(\rho c_p)_p$ where $(\rho c_p)_p$ is the heat capacity of the nanofluid and $(\rho c_p)_p$ is the heat capacity of the nanoparticle, respectively.

In order to find the similarity solution of Equations 1- 6, the similarity transformation parameters are introduced as follows

$$\psi=Ax(\nu/t)^{1/2}f(\eta),\ \theta(\eta)=\frac{T-T_\infty}{T_w-T_\infty},\ \varphi(\eta)=\frac{C-C_\infty}{C_\infty},\ \eta=\frac{y}{(\nu t)^{1/2}} \tag{7}$$

where η is the dimensionless similarity variable, the prime denotes differentiation with respect to η,ψ is the stream function which defines $\mu=\partial\psi/\partial y=(Ax/t)f(\eta)$ and $v=-\partial\psi/\partial_x=-A(v/t)^{1/2}f(\eta)$, $f(\eta)$,$\theta(\eta)$and $\phi(\eta)$ are dimensionless stream, temperature and concentration functions of the fluid in the boundary layer, respectively and v_w is represented as $v_w=-A(v/t)^{1/2}s$, where s is the constant mass flux which s>0 for suction and s<0 for injection.

Using similarity transformation Equation 7, the partial differential Equation 1- 5 are transformed to ordinary differential Equation 8-10 subject to boundary conditions

$$f'''+A\left(ff''-f'^2\right)+f'+\frac{\eta}{2}f''=0, \tag{8}$$

$$\frac{1}{\Pr}\theta''+\left(Af+\frac{\eta}{2}\right)\theta'+Nb\phi'\theta'+Nt\theta'^2+Df\phi''=0, \tag{9}$$

$$\phi''+Le\left(Af+\frac{\eta}{2}\right)\phi'+\frac{Nt}{Nb}\theta''+LeSr\theta''=0, \tag{10}$$

$f(0)=s, f\eta(0)=\varepsilon, \theta(0)=1, Nb\phi(0)+Nt\eta(0)=0,$

$$f\eta(\eta)\to 0,\ \theta(\eta)\to 0,\ \phi(\eta)\to 0 \text{ as } \eta\to\infty \tag{11}$$

Where *Pr* is Prandtl number, is Brownian motion parameter, *Nt* is the thermophoresis parameter, *Le* is Lewis number, *Df* is Dufour number and *Sr* is the Soret number which are defined as

$$\Pr=\frac{\nu}{\alpha},\ Nb=\frac{\tau}{\nu}D_B C_\infty,\ Nt=\frac{\tau}{\nu}\frac{D_T(T_w-T_\infty)}{T_\infty},\ Le=\frac{\nu}{D_B},$$
$$Df=\frac{D_B k_T C_\infty}{\nu c_s c_p(T_w-T_\infty)},\ Sr=\frac{D_B k_T(T_w-T_\infty)}{\nu T_m C_\infty}. \tag{12}$$

The skin friction coefficient and the local Nusselt number are the quantities of physical interest in this problem and defined as

$$C_f=\frac{\tau_w}{\rho u_w^2}\ \text{and}\ Nu_x=\frac{xq_w}{k(T_w-T_\infty)}, \tag{13}$$

Where τ_w *and* q_w are the shear stress and heat flux at the surface, respectively as given by

$$\tau_w=\mu\left(\frac{\partial u}{\partial y}\right)_{y=0}\ \text{and}\ q_w=-k\left(\frac{\partial T}{\partial y}\right)_{y=0}, \tag{14}$$

Where μ is the dynamic viscosity of the fluid and *k* is the thermal conductivity of the nanofluid. Equations 7, 13, 14 we obtain

$$C_f\mathrm{Re}_x^{1/2}=A^{-1/2}f\eta\eta\,(0) \tag{15}$$
$$\mathrm{Nu}_x\mathrm{Re}_x^{-1/2}=-A^{-1/2}\theta\eta\ (0),$$

Where $\mathrm{Re}_x=u_w/\nu$ represents local Reynold number.

Stability Analysis

Weidman et al. [32], and Roşca and Pop [39,40] have shown that the lower branch solutions are unstable (not physically realizable), while the upper branch solutions are stable (physically realizable). We test these features by considering Equations 1-5. Thus, we introduce the new dimensionless time variable $\tau=\ln(t/t_o)$, where t_o is a characteristic time. The use of τ is associated with an initial value problem and is consistent with the question of which solution will be obtained in practice (physically realizable). Using the variables τ and Equation 7, we have

$$u=\frac{Ax}{t}\frac{\partial f}{\partial\eta}(\eta,\tau),\quad v=-A\left(\frac{\nu}{t}\right)^{1/2}f(\eta,\tau),\quad \theta(\eta,\tau)=\frac{T-T_\infty}{T_w-T_\infty},\quad \varphi(\eta,\tau)=\frac{C-C_\infty}{C_\infty},$$
$$\eta=\frac{y}{(\nu t)^{1/2}},\quad \tau=\ln(t/t_0). \tag{16}$$

As in Weidman et al. [32], we introduce the new variable $\tau=ln(t/t_o)$ as it is associated with initial value problem, where t_o is a characteristic time and we take $t_o=1$ so we have $\tau=ln(t)$ Thus, Equations 1-5 can be written as

$$\frac{\partial^3 f}{\partial\eta^3}+A\left[f\frac{\partial^2 f}{\partial\eta^2}-\left(\frac{\partial f}{\partial\eta}\right)^2\right]+\frac{\partial f}{\partial\eta}+\frac{\eta}{2}\frac{\partial^2 f}{\partial\eta^2}-\frac{\partial^2 f}{\partial\eta\,\partial\tau}=0, \tag{17}$$

$$\frac{1}{\Pr}\frac{\partial^2\theta}{\partial\eta^2}+\left(Af+\frac{\eta}{2}\right)\frac{\partial\theta}{\partial\eta}+Nb\frac{\partial\varphi}{\partial\eta}\frac{\partial\theta}{\partial\eta}+Nt\left(\frac{\partial\theta}{\partial\eta}\right)^2+Df\frac{\partial^2\varphi}{\partial\eta^2}-\frac{\partial\theta}{\partial\tau}=0, \tag{18}$$

$$\frac{\partial^2\varphi}{\partial\eta^2}+Le\left(Af+\frac{\eta}{2}\right)\frac{\partial\varphi}{\partial\eta}+\left(LeSr+\frac{Nt}{Nb}\right)\frac{\partial^2\theta}{\partial\eta^2}-Le\frac{\partial\varphi}{\partial\tau}=0, \tag{19}$$

subject to the initial and boundary conditions

$$f(0,\tau)=s,\quad \frac{\partial f}{\partial\eta}(0,\tau)=\varepsilon,\quad \theta(0,\tau)=1,\quad Nb\frac{\partial\varphi}{\partial\eta}(0,\tau)+Nt\frac{\partial\theta}{\partial\eta}(0,\tau)=0,$$
$$\frac{\partial f}{\partial\eta}(\eta,\tau)\to 0,\quad \theta(\eta,\tau)\to 0,\quad \varphi(\eta,\tau)\to 0\quad \text{as}\quad \eta\to\infty. \tag{20}$$

To determine the stability of the solution $f=f_0(\eta)$, $\theta=\theta_0(\eta)$ and $\phi=\phi_0(\eta)$ satisfying the boundary-value problem Equation 8-11, we write Weidman et al. [32], and Roşca and Pop [39,40])

$$F(\eta,\tau)=f_0(\eta)+e^{-\gamma\tau}F_0(\eta),\ \theta(\eta,\tau)=\theta_0(\eta)+e^{-\gamma\tau}G_0(\eta), \quad (21)$$

$$\Phi(\eta,\tau)=\phi 0(\eta)+e^{-\gamma\tau}H_0(\eta),$$

Where γ is an unknown eigenvalue parameter, and $f_0(\eta)$, $G_0(\eta)$ and $H_0(\eta)$ are small relative to $f_0(\eta)$, $\theta_0(\eta)$ and $\phi_0(\eta)$ Substituting Equation 21 into Equation 17-19, and take $\tau=0$, we obtain the following linear eigenvalue problem

$$F_0'''+\left(Af_0+\frac{\eta}{2}\right)F_0''+(1-2Af_0'+\gamma)F_0'+Af_0''F_0=0, \quad (22)$$

$$\frac{1}{\Pr}G_0''+\left(Af_0+Nb\phi_0'+2Nt\theta_0'+\frac{\eta}{2}\right)G_0'+\theta_0'F_0+Nb\,\theta_0'H_0' + Df\,H_0''+\gamma G_0=0, \quad (23)$$

$$H_0''+Le\left(Af_0+\frac{\eta}{2}\right)H_0'+\phi_0'F_0+\left(LeSr+\frac{Nt}{Nb}\right)G_0''+Le\,\gamma H_0=0, \quad (24)$$

subject to the boundary conditions

$$F_0(0),\ F_0\eta(0)=0,\ G_0(0)=0,\ Nb\,H_0\eta(0)+Nt\,G_0\eta(0)=0,$$

$$F_0\eta(\eta)\to 0,\ G_0(\eta)\to 0,\ H_0(\eta)\to 0 \text{ as } \eta\to\infty \quad (25)$$

Solving the eigenvalue problem Equations 22-25 we obtain an infinite number of eigenvalues $\gamma_1<\gamma_2<\gamma_3<\ldots$. If the smallest eigenvalue is positive the flow is stable and if the smallest eigenvalue is negative the flow is unstable.

According to Harris et al. [41], the range of possible eigenvalues can be determined by relaxing a boundary condition on $f_0(\eta)$, $G_0(\eta)$ or $H_0(\eta)$. For the present problem, we relax the boundary condition $F_0\eta(\eta)\to 0$ as $\eta\to\infty$ and for a fixed value of γ we solve the system of Equations 22-24 subject to [25] along with the new boundary condition $F_0\eta\eta(0)=1$.

Results and Discussion

In order to obtain numerical results of the reduced skin friction coefficient $F_0\,\eta\eta\,(0)$ and reduced Nusselt number $-\theta=(0)$ with the effect of various physical parameters, we fixed some parameter values such as Prandtl number Pr=0.71 (air), Lewis number Le=1, Brownian motion parameter Nb=0.5 and thermophoresis parameter Nt=0.5 and solve the system of ordinary differential Equation 8-10 subject to boundary conditions Equation 11 by applying bvp4c in Matlab. Further, the presence of Soret and Dufour parameters are now considered and the values of Soret, Sr and Dufour, D_f are chosen in such way so that the mean temperature T_m remains as a constant (see El-Kabeir [6]). A comparison with previous results (see Bachok et al. [38]) with the absence of Soret and Dufour effects is made in order to validate the numerical computation where the comparison shows a good agreement as can be seen in Table 1. Apart from that, the presence of Soret and Dufour effects doesn't affect the range of solution of ε since the value of ε_c are identical with the absence of both effects.

The effects of mass suction/ injection parameters on the reduced skin friction coefficient $F_0\eta\eta\,(0)$ and reduced Nusselt number $-\theta=\eta(0)$ with stretching/ shrinking parameter ε, when A=1 are shown in Figures 1 and 2. Moreover, Figures 3 and 4 present the effects of unsteadiness parameter, A on those two quantities physical of interest. Based on the Figures 3 and 4 the dual solutions are found when $\varepsilon\le\varepsilon_c$ and no solution can be obtained when $\varepsilon>\varepsilon_c$. From these figures, the range of solutions, $|\varepsilon_c|$ are expanded as the value of A and s increased.

Figures 1 and 4 show that the reduced skin friction coefficient increases when the ε decreases whereas the reduced Nusselt number slightly decreases for the same decreasing parameter. Besides, the range of solutions for higher value of mass flux parameter are wider compared to smaller value as can be noticed in Figures 1 and 2. Likewise Figures 3 and 4 demonstrates the ranges of solution for larger value of unsteadiness parameter are broader than lower value of A with ε.

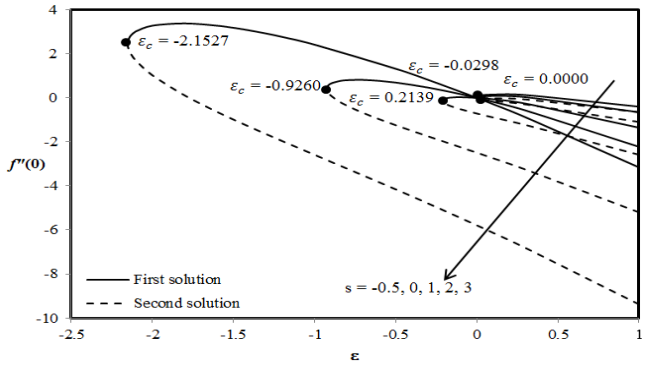

Figure 1: Variation of reduced skin friction coefficient with ε.

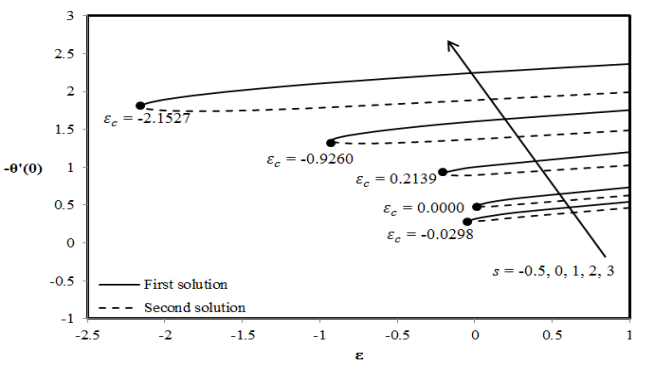

Figure 2: Variation of reduced Nusselt number with for different values of *s when Nt=Nb=0.5 Df=0.15, Le=1, Sr=0.4, A=1 and Pr=0.71.*

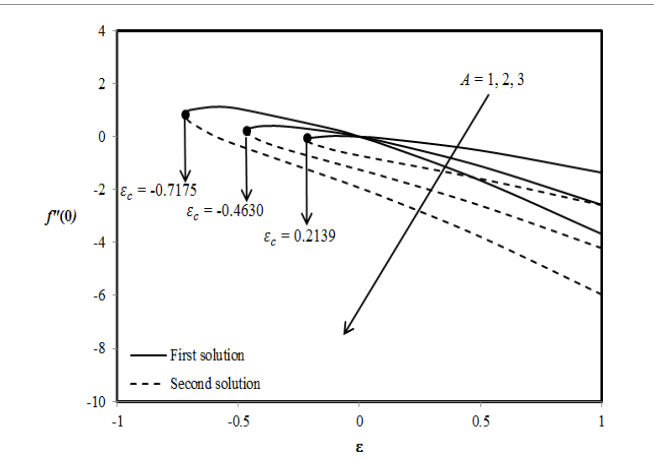

Figure 3: Variation of reduced skin friction coefficient with ε for different values of when *s=1*.

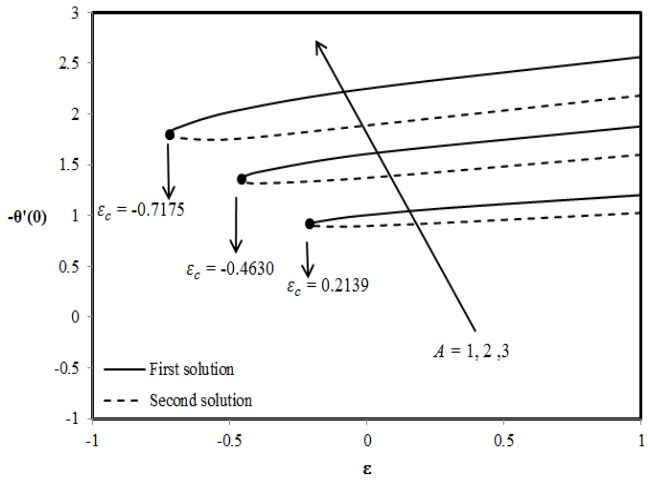

Figure 4: Variation of reduced Nusselt number with ε for different values of *A* when *Nt=Nb=0.5, Df=0.15, Le=1, Sr=0.4, A=1, s=1* and *Pr=0.71*.

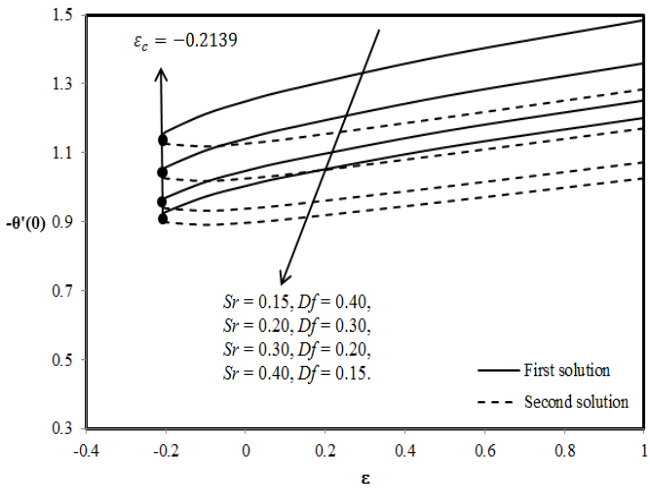

Figure 5: Variation of reduced Nusselt number with ε for different values of *Sr* and *Df* when *A=1*, *Nt=Nb=0.5, Le=1, s=1* and *Pr=0.71*.

Figure 1 illustrates that as mass flux increases, the values of $F_0\,\eta\eta(0)$ are found decelerated for $\varepsilon>0$ (stretching sheet) and opposite trend can be observed when ε (shrinking sheet). Moreover, the values $-\theta(0)$ are larger for higher values of mass flux parameter *s* as depicts in Figures 2 and 3 shows that a hike in unsteadiness parameter increases the skin friction at the surface for shrinking sheet but for stretching sheet $\varepsilon>0$, the skin friction declines. It is also can be mentioned from Figure 4, the $\varepsilon<0$ accelerating unsteadiness parameter increases the reduced Nusselt number which proportional to the heat transfer rate at the surface.

Figure 5 represents the effect of different values of Soret *Sr* and Dufour D_f on reduced Nusselt number with. From the figure, it is found that the increase in *Sr* (or decreasing D_f) doesn't expand the range of solution where the dual solutions are found when $\varepsilon>\varepsilon_c$=-0.2139 while no solution is reported when $\varepsilon>\varepsilon_c$=-0.2139. Apart from that, the increase in *Sr* (or decreasing D_f)) decreases the reduced Nusselt number and the decrease in ε decreases the reduced Nusselt number. This shows that the heat transfer rate at the surface decreases for higher Soret (or lower Dufour) parameter.

The effects of Soret and Dufour with mass flux parameter *s* on reduced Nusselt number, $-\theta\ \eta\ (0)$ is shown in Figure 6. The increasing

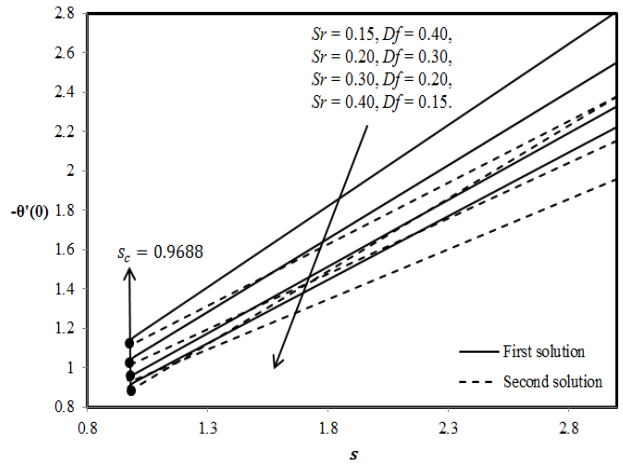

Figure 6: Variation of reduced Nusselt number with *s* for different values of *Sr* and *Df* when, *Nt=Nb=0.5, Le=1, A=1, Pr=0.71* and ε*=-0.2* (Shrinking).

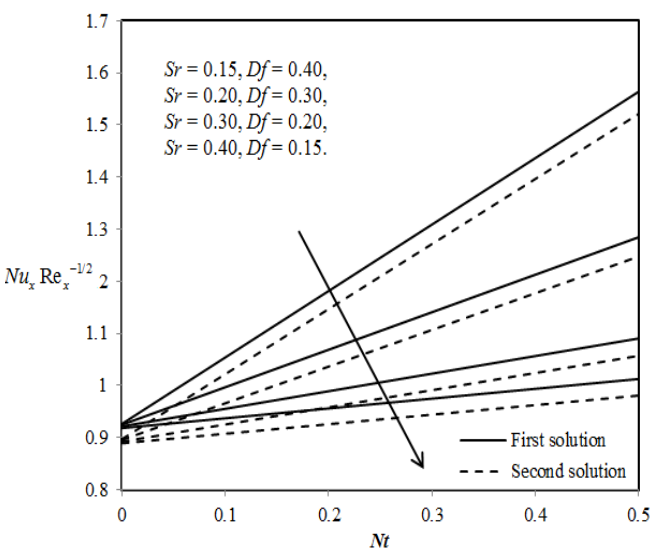

Figure 7: Variation of local Nusselt number with *Nt* for different values of *Sr* and *Df* when, *Nb=0.3*, *Le=1, A=1, Pr=0.71* and ε*=-0.2* (Shrinking).

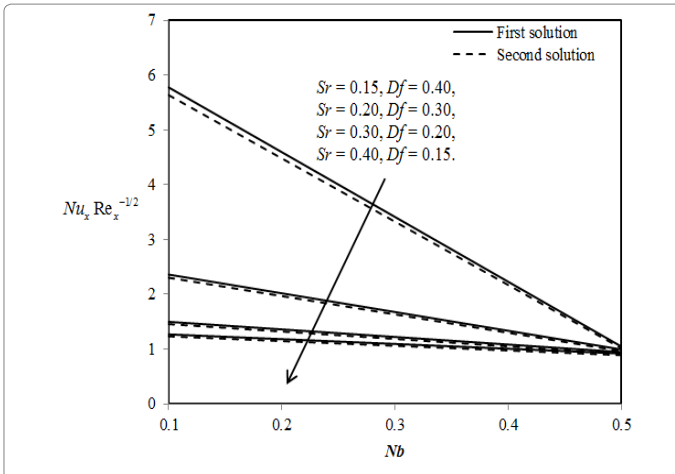

Figure 8: Variation of local Nusselt number with *Nb* for different values of *Sr* and *Df* when, *Le=1, A=1, Pr=0.71* and ε*=-0.2* (Shrinking).

Soret (or decreasing Dufour) decreases the reduced Nusselt number which means the rate of heat transfer decreases for higher Soret (or lower Dufour) parameter. While for increasing mass flux parameter s the reduced Nusselt number is increasing for both solutions. The presence of Soret and Dufour effects is found doesn't change the range of the solutions where the dual solutions exist when $s>sc$=0.9688 and no solution can be obtained when $s<sc$=0.9688. In addition, it is revealed that the solutions exist only for $s>0$ which represents mass suction parameter. Hence, the dual solutions can be obtained when the mass suction parameter is considered the study and no solution is existed as mass injection parameter is taken into account.

The variations of local Nusselt number with thermophoresis parameter Nt and Brownion motion parameter Nb for several values of Soret and Dufour are shown in Figures 7 and 8 respectively. Figure 7 shows that the local Nusselt number decreases with increasing Soret (or decreasing Dufour) which indicates the heat transfer rate at the surface decreases when the heat flux due to the concentration gradient is increased or mass flux generated by temperature gradient is decreased. In addition, the local Nusselt number is increased when the thermophoresis parameter increases. Physically, the rate of heat transfer is found increased as the migration of the particles increase. Figure 7 demonstrates the local Nusselt number which represents rate of heat transfer decreases when the Soret (Dufour) parameter increases (decreases) as well as the Brownion motion parameter Nb increases.

Figures 8-21 present the effect of unsteadiness, mass flux, stretching/shrinking velocity, and Sufor and Dufour parameters on velocity, temperature and concentration profiles. As can be seen in these profiles, the boundary conditions Equation 11 are satisfied asymptotically. Besides that, the dual solutions are obtained which support the variations of reduced skin friction coefficient as well as reduced Nusselt number as presented in Figures 1-8. These profiles also show that the boundary layer thicknesses for first solution are smaller than second solution in each profile. The effect of increasing Sr (or decreasing D_f) on temperature and concentration profiles can be observed in Figures 18 and 19 for shrinking parameter and Figures 20 and 21 for stretching parameter. It is found that increasing Sr (or decreasing D_f) decreases the temperature and the concentration at the surface for both stretching and shrinking cases.

The stability of dual solutions can be determined by performing the stability analysis and has been solved using bvp4c to obtain the smallest eigenvalue γ for some values of mass suction parameter s and shrinking parameter γ as can be seen in Table 2. According to the table,

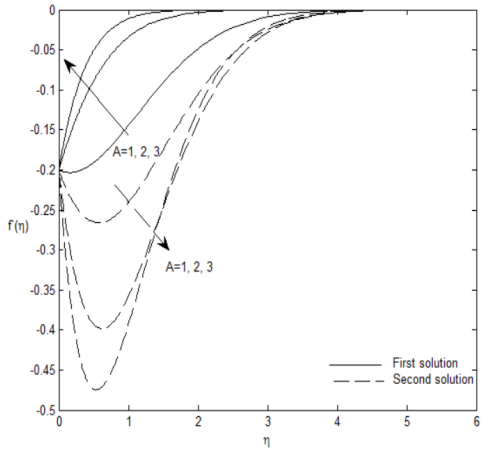

Figure 9: Velocity profile for different values of A when $s=1$ and $\varepsilon=-0.2$ (Shrinking).

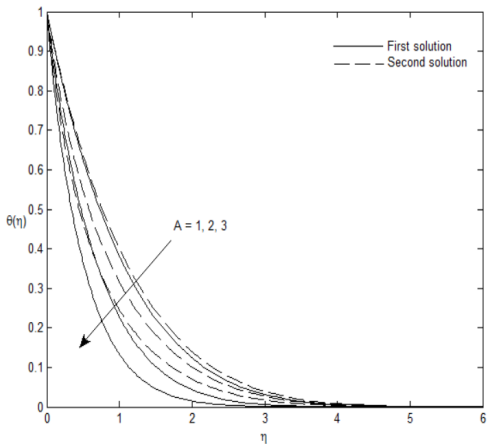

Figure 10: Temperature profile for different values of A when $Nt=Nb=0.5$, $Le=1$, $A=1$, $Df=0.15$, $Le=1$, $Sr=0.4$, $Pr=0.71$ and $\varepsilon=-0.2$ (Shrinking).

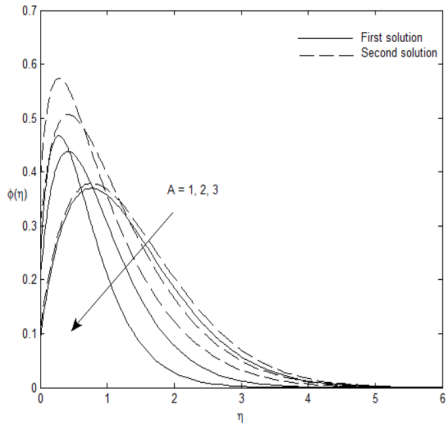

Figure 11: Concentration profile for different values of A when when $Nt=Nb=0.5$, $Le=1$, $A=1$, $Df=0.15$, $Le=1$, $Sr=0.4$, $Pr=0.71$ and $\varepsilon=-0.2$ (Shrinking).

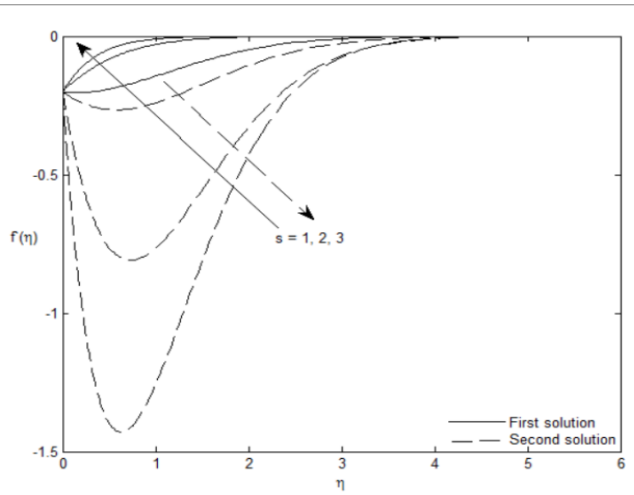

Figure 12: Velocity profile for different values of s when $A=1$ and $\varepsilon=-0.2$ (Shrinking).

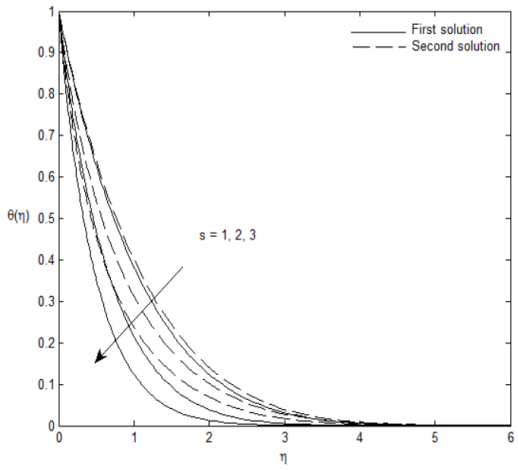

Figure 13: Temperature profile for different values of s when Concentration profile for different values of *A* when when *Nt=Nb=0.5, Df=0.15, Le=1, Sr=0.4, A=1, Pr=0.71* and *ε=-0.2* (Shrinking).

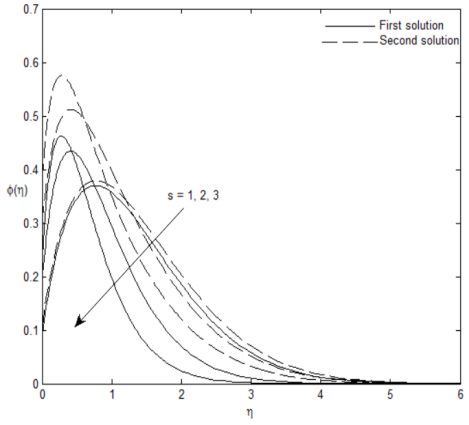

Figure 14: Concentration profile for different values of *s* when *Nt=Nb=0.5, Df=0.15, Le=1, Sr=0.4, A=1, Pr=0.71 and ε=-0.2* (Shrinking).

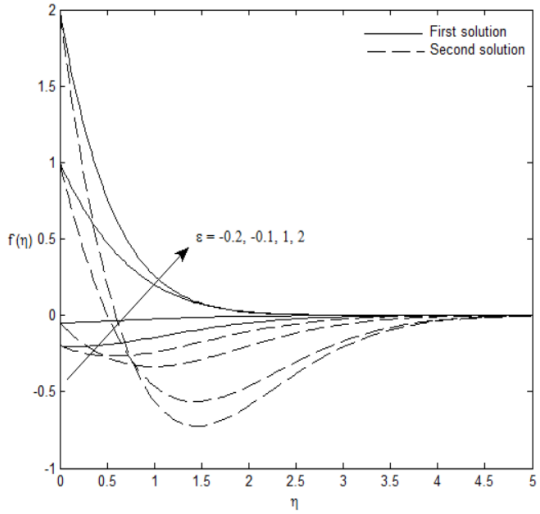

Figure 15: Velocity profile for different values of $\mathcal{E}$ when *A=1 and s=1*.

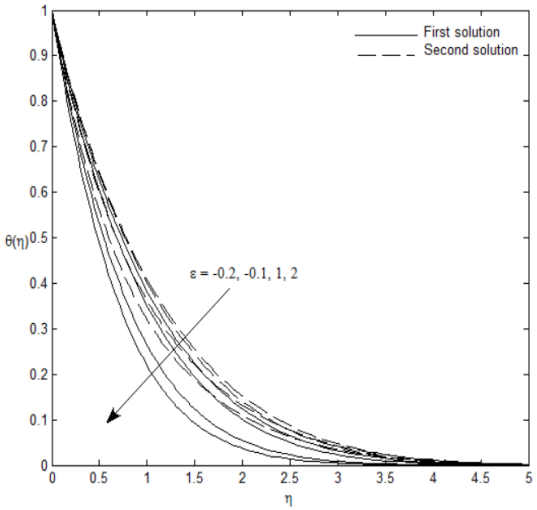

Figure 16: Temperature profile for different values of when *Nt=Nb=0.5, Df=0.15, Le=1, Sr=0.4, A=1, Pr=0.71* and *s=1*.

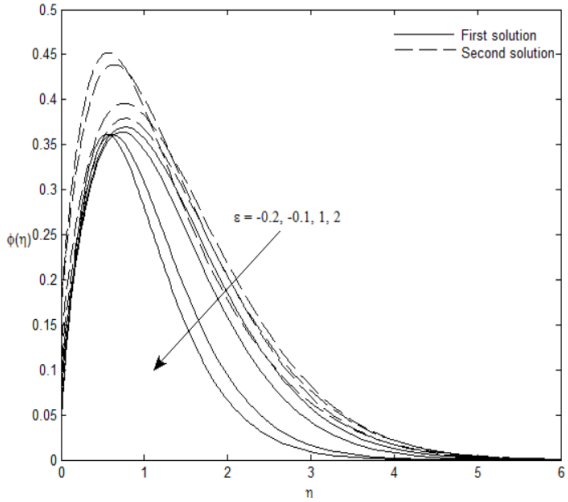

Figure 17: Concentration profile for different values of when *Nt=Nb=0.5, Df=0.15, Le=1, Sr=0.4, A=1, Pr=0.71* and *s=1*.

the smallest eigenvalues for upper branch solution is positive while for lower branch solution is negative. Thus, the first solutions with positive smallest eigenvalues indicate that the solution is stable and physically reliable while second solution is unstable and physically unreliable.

Conclusion

The effect of Soret and Dufour parameters as well as the unsteadiness, mass flux, thermophoresis, Brownian motion parameters on heat transfer characteristics for unsteady boundary layer flow over stretching/shrinking sheet in nanofluid is investigated numerically. It is found that the dual solutions are obtained in this study and presented graphically for reduced skin friction coefficient, reduced Nusselt number as well as the velocity, temperature and nanoparticle volume fraction profiles. The different values of Soret and Dufour parameters are found doesn't affect the range of ε and s parameters since the critical value of ε (ε_c=-0.2139) and s (s_c=0.9688) are unchanged even though the values of Soret and Dufour parameter are different. In contrast, the higher values of unsteadiness and mass flux parameters expand range of where the dual

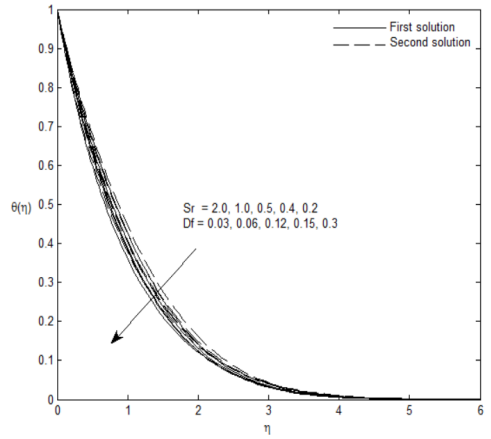

Figure 18: Temperature profile for different values of *Sr* and *Df* when *Nt=Nb=0.5, Le=1, s=1, A=1, Pr=0.71 and* ε*=-0.2* (Shrinking).

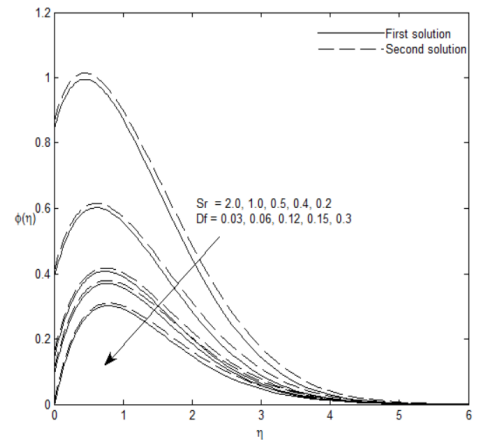

Figure 19: Concentration profile for different values of *Sr* and *Df* when *Nt=Nb=0.5, Df=0.15, Le=1, s=1, A=1, Pr=0.71 and* ε*=-0.2* (Shrinking).

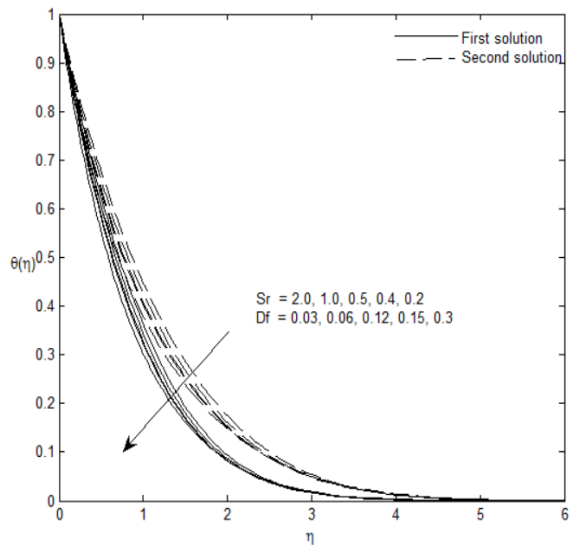

Figure 20: Temperature profile for different values of *Sr* and *Df* when *Nt=Nb*=0.5, *Le*=1, *s*=1, *A*=1, *Pr=0.71 and* ε*=-0.2* (stretching).

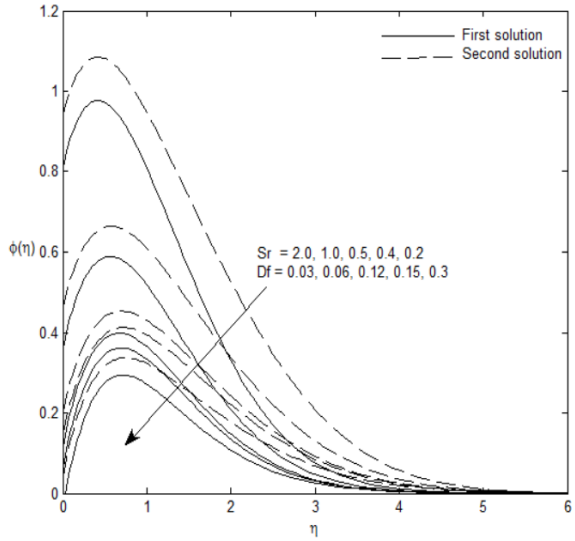

Figure 21: Concentration profile for different values of *Sr* and *Df* when *Nt=Nb*=0.5, *Le*=1, *s*=1, *A*=1, *Pr*=0.71 *and* ε=-0.2 (stretching).

Df	*Sr*	*s*	Bachok et al. [38] ε_c	Present results ε_c
0	0	0	0.0000	0.0000
		1	-0.2138	-0.2139
		2	-0.9259	-0.9260
0.15	0.4	0	-	0.0000
		1	-	-0.2139
		2	-	-0.9260

Table 1: Comparison numerical values of critical epsilon, ε_c for different *s* when *Nt=Nb*=0.5, *Le*=2, *A*=1 and *Pr*=0.71.

s	ε_c	ε	γ (First solution)	γ (Second solution)
1	-0.2139	-0.2135	0.0314	-0.0311
		-0.213	0.0472	-0.0466
		-0.21	0.0991	-0.0964
2	-0.9260	-0.926	0.0024	-0.0007
		-0.92	0.1509	-0.1468
		-0.91	0.2482	-0.2373

Table 2: The smallest eigen values *γ* for some values of s and when *Nt=Nb*=0.5, *Df*=0.15, *Le*=1, *Sr*=0.4, *A*=1 and *Pr*=0.71.

solutions can be obtained when ε*>-22* for different mass flux parameter and ε*>- 88* for various unsteadiness parameter. The stability of the solutions is performed where the first solution is found stable while the second solution is unstable.

References

1. Joly F, Vasseur P, Labrosse G (2000) Soret-driven thermosolutal convection in a vertical enclosure. Int. Commun. Heat Mass Transf 27: 755-764.
2. Mansour A, Amahmid A, Hasnaoui M, Bourich M (2006) Multiplicity of solutions induced by thermosolutal convection in a square porous cavity heated from below and submitted to horizontal concentration gradient in the presence of Soret effect. Num. Heat Transfer 49: 69-94.
3. Chamkha AJ, Rashad AM (2014) Unsteady heat and mass transfer by MHD mixed convection flow from a rotating vertical cone with chemical reaction and Soret and Dufour effects. Canadian J. Chem. Engng 92: 758-767.
4. Kafoussias NG, Williams EW (1995) Thermal-diffusion and diffusion-thermo effects on mixed free-forced convective and mass transfer boundary layer flow with temperature dependent viscosity. Int. J. Engng. Sci 33: 1369-1384.

5. Alam MR, Samad M (2006) Dufour and Soret effects on unsteady MHD free convection and mass transfer flow past a vertical porous plate in a porous medium. Nonlinear Anal. Model. Control 119: 217-226.

6. Kabeir SME (2011) Soret and Dufour effects on heat and mass transfer due to a stretching cylinder saturated porous medium with chemically-reactive species. Latin Am. Appl. Res 41: 331-337.

7. Choi SUS (1995) Enhancing thermal conductivity of fluids with nanoparticles. In: Proceedings of the 1995 ASME International Mechanical Engineering Congress and Exposition, FED 231/MD, Vol. 66, ASME, San Francisco, CA, pp: 99-105.

8. Khanafer K, Vafai K, Lightstone M (2003) Buoyancy driven heat transfer enhancement in a two-dimensional enclosure utilizing nanofluids. Int. J. Heat Mass Transfer 46: 3639-3653.

9. Tiwari RK, Das MK(2007) Heat transfer augmentation in a two-sided lid-driven differentially heated square cavity utilizing nanofluids. Int. J. Heat Mass Transfer 50: 2002-2018.

10. Oztop HF, Abu NE (2008) Numerical study of natural convection in partially heated rectangular enclosures filled with nanofluids. Int. J. Heat Fluid Flow 29: 1326-1336.

11. Lai FH, Yang YT (2011) Lattice Boltzmann Simula tion of Natural Convection Heat Transfer of Al2O3/water Nanofluids in a Square Enclosure. Int. J. Therm. Sci 50: 1930-1941.

12. Aminossadati SM, Ghasemi B (2011) Natural convection of water-CuO nanofluid in a cavity with two pairs of heat source-sink. Int. Commun. Heat Mass Transf 38: 672-678.

13. Buongiorno J (2006) Convective transport in nanofluids. J. Heat Transfer 128: 240-250.

14. Kuznetsov AV, Nield DA (2010) Natural convective boundary-layer flow of a nanofluid past a vertical plate. Int. J. Thermal Sci. 49: 243-247.

15. Mansur S, Ishak A (2013) The flow and heat transfer of a nanofluid past a stretching/ shrinking sheet with a convective boundary condition. Abstract and Applied Analysis 2013: 1-9.

16. Kuznetsov AV, Nield DA (2013) The Cheng-Minkowycz problem for natural convective boundary layer flow in a porous medium saturated by a nanofluid: A revised model. Int. J. Heat Mass Transfer 65: 5792-5795.

17. Nemati H, Farhadi M, Sedighi K, Fattahi E, Darzi AAR (2010) Lattice Boltzmann simulation of nanofluid in lid-driven cavity. Int. Commun. Heat Mass 37: 1528-1534.

18. Cimpean D, Pop I (2012) Fully developed mixed convection flow of a nanofluid through an inclined channel filled with a porous medium. Int. J. Heat Mass Transfer 55: 907-914.

19. Jou RY, Tzeng SC (2006) Numerical research of nature convective heat transfer enhancement filled with nanofluids in rectangular enclosures. Int. Comm. Heat Mass Transfer 33: 727-736.

20. Das SK, Choi SUS, Yu W, Pradeep T (2008) Nanofluids: Science and Technology, Wiley, New Jersey, USA, p: 416.

21. Kleinstreuer C, Li J, Koo J (2008) Microfluidics of nano-drug delivery. Int. J. Heat Mass Transfer 51: 5590-5597.

22. Kakac S, Pramuanjaroenkij A (2009) Review of convective heat transfer enhancement with Nano fluids. Int. J. Heat Mass Transfer 52: 3187-3196.

23. Wong KV, Leon OD (2010) Applications of nanofluids: current and future. Adv. Mech. Engg. 519: 659.

24. Wen D, Corr M, Hu X, Lin G (2011) Boiling heat transfer of nanofluids: The effect of heating surface modification. Int. J. Therm. Sci. 50: 480-485.

25. Jaluria Y, Manca O, Poulikakos D, Vafai K, Wang L (2012) Heat transfer in nanofluids. Adv. Mech. Engng 972: 973.

26. Mahian O, Kianifar A, Kalogirou SA, Pop I, Wongwises S (2013) A review of the applications of nanofluids in solar energy. Int. J. Heat Mass Transfer 57: 582-594.

27. Nield DA, Bejan A (2013) Convection in Porous Media. 4th edn. Springer, New York, USA.

28. Sheikholeslami M, Ganji DD (2016) Nanofluid convective heat transfer using semianalytical and numerical approaches: a review. J. Taiwan Inst. Chem. Eng 65: 43-77.

29. Shenoy A, Sheremet MA, Pop I (2016) Convective Flow and Heat Transfer past Wavy Surfaces: Viscous Fluids, Porous Media and Nanofluids, CRC Press, Taylor & Francis Group, New York.

30. Merkin JH (1980) Mixed convection boundary layer flow on a vertical surface in a saturated porous medium. J. Engng. Math 14: 301-313.

31. Ishak A (2014) Dual solutions in mixed convection boundary layer flow : A stability analysis. Int. J. Math. Comput. Phys. Quantum Eng. 8: 1131-1134.

32. Weidman PD, Kubitschek DG, Davis AMHJ (2006) The effect of transpiration on self-similar boundary layer flow over moving surfaces. Int J Eng Sci. 44: 730-737.

33. Aleng NL, Bachok N, ArifinM N (2014) Boundary Layer Flow of a Nanofluid and Heat Transfer over an Exponentially Shrinking Sheet: Copper-Water. Math. Comput. Methods Sci. Eng 74: 137-142.

34. Nazar R, Noor A, Jafar K, Pop I (2014) Stability Analysis of Three-Dimensional Flow and Heat Transfer over a Permeable Shrinking Surface in a Cu-Water Nanofluid. World Acad Sci Eng Technol Int J Math Comput Stat Nat Phys Eng 1: 780-786.

35. Hafidzuddin E, Nazar R, Arifin NM, Pop I (2015) Stability Analysis of Unsteady Three-Dimensional Viscous Flow Over a Permeable Stretching / Shrinking Surface. J. Qual. Meas. Anal. 11: 19-31.

36. Bachok N, Najib N, Arifin N, Senu N (2016) Stability of Dual Solutions in Boundary Layer Flow and Heat Transfer on a Moving Plate in a Copper-Water Nanofluid with Slip Effect. WSEAS Trans. Fluid Mech. 11: 151-158.

37. Najib N, Bachok N, Arifin N, Senu N (2017) Boundary Layer Flow and Heat Transfer of Nanofluids over a Moving Plate with Partial Slip and Thermal Convective Boundary Condition : Stability Analysis. Int. J. Mech. 11: 18-24.

38. Bachok N, Ishak A, Pop I (2013) Unsteady boundary-layer flow and heat transfer of a nanofluid over a permeable stretching/shrinking sheet. Int. J. Heat Mass Transf. 55: 2102-2109.

39. Rosca AV, Pop I (2013) Flow and heat transfer over a vertical permeable stretching/ shrinking sheet with a second order slip. Int. J. Heat Mass Transfer 60: 355-364.

40. Rosca NC, Pop I (2013) Mixed convection stagnation point flow past a vertical flat plate with a second order slip: heat flux case. Int. J. Heat Mass Transfer 65: 102-109.

41. Harris SD, Ingham DB, Pop I (2009) Mixed convection boundary-layer flow near the stagnation point on a vertical surface in a porous medium: Brinkman model with slip. Transport Porous Med 77: 267-285.